



Dissolution corrosion of 316L austenitic stainless steels in contact with static liquid lead-bismuth eutectic (LBE) at 500 °C



Konstantina Lambrinou^{a,*}, Evangelia Charalampopoulou^{a,b}, Tom Van der Donck^c, Rémi Delville^a, Dominique Schryvers^b

^a SCK-CEN, Boeretang 200, 2400 Mol, Belgium

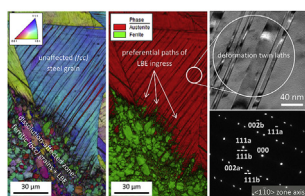
^b University of Antwerp, Electron Microscopy for Materials Science (EMAT), Groenenborgerlaan 171, 2020 Antwerpen, Belgium

^c KU Leuven, Department of Materials Engineering, Kasteelpark Arenberg 44, 3001 Leuven, Belgium

HIGHLIGHTS

- Dissolution corrosion was more severe in cold-deformed than solution-annealed 316L steels.
- LBE penetration occurred along preferential paths in the steel microstructure.
- The maximum dissolution rate was inversely proportionate to the depth of dissolution.

GRAPHICAL ABSTRACT



ARTICLE INFO

Article history:

Received 11 September 2016

Received in revised form

2 April 2017

Accepted 2 April 2017

Available online 10 April 2017

Keywords:

Stainless steel

SEM

TEM

De-alloying

Intergranular corrosion

Pitting corrosion

ABSTRACT

This work addresses the dissolution corrosion behaviour of 316L austenitic stainless steels. For this purpose, solution-annealed and cold-deformed 316L steels were simultaneously exposed to oxygen-poor ($<10^{-8}$ mass%) static liquid lead-bismuth eutectic (LBE) for 253–3282 h at 500 °C. Corrosion was consistently more severe for the cold-drawn steels than the solution-annealed steel, indicating the importance of the steel thermomechanical state. The thickness of the dissolution-affected zone was non-uniform, and sites of locally-enhanced dissolution were occasionally observed. The progress of LBE dissolution attack was promoted by the interplay of certain steel microstructural features (grain boundaries, deformation twin laths, precipitates) with the dissolution corrosion process. The identified dissolution mechanisms were selective leaching leading to steel ferritization, and non-selective leaching; the latter was mainly observed in the solution-annealed steel. The maximum corrosion rate decreased with exposure time and was found to be inversely proportional to the depth of dissolution attack.

© 2017 Elsevier B.V. All rights reserved.

1. Introduction

One of the principal challenges in the development of Gen-IV lead-cooled fast reactors (Gen-IV LFRs) is the inherent corrosiveness of the primary heavy liquid metal coolant, such as lead (Pb) and lead-bismuth eutectic (LBE), for structural and cladding candidate steels considered for the construction of such reactor systems [1–5]. The inherent corrosiveness of lead-alloys (Pb, LBE,

Pb-Li) is also a concern in fusion (tritium breeding blanket concept), in concentrated solar power (CSP) systems using heavy liquid metals [6], and in accelerator-driven systems (ADS) that use heavy liquid metals as spallation targets. An example of ADS technology currently under development at SCK•CEN, Belgium, is the flexible fast-spectrum irradiation facility MYRRHA (multi-purpose hybrid research reactor for high-tech applications), which will use liquid LBE as primary coolant and spallation target [7]. The mitigation of undesirable liquid metal corrosion (LMC) effects in MYRRHA is based on three main pillars, i.e., moderate operating temperatures (<450 °C), active oxygen control and understanding of the steel-

* Corresponding author. SCK-CEN, Boeretang 200, B-2400 Mol, Belgium.

E-mail address: klambrin@sckcen.be (K. Lambrinou).

specific LMC mechanisms. Active oxygen control strives to form a protective oxide scale on the steel surface by dissolving precise amounts of oxygen in the heavy liquid metal (HLM) coolant [3,5,8–10]. The concentration of dissolved oxygen in the HLM must ensure the formation of protective oxides on the steels without oxidising the HLM itself (too high oxygen potential) [11]. If, for any reason, the oxygen potential drops below a certain level, the oxide scales will be reduced and the steel will come into direct contact with the HLM [11]; such eventuality is undesirable, as it will result in the steel dissolution corrosion. Dissolution corrosion of austenitic stainless steels, such as the 316L steel studied in this work, involves the loss of steel alloying elements into the heavy liquid metal and the progressive LBE penetration into the steel [12–18]; moreover, LBE dissolution attack can be locally-enhanced, creating deep 'pits' that might result in the premature breaching of thin-walled components, such as heat exchanger and fuel cladding tubes [12,19,20].

Since the MYRRHA candidate structural steel is the 316L stainless steel, it is important for the development of this system to understand all aspects of the LMC behaviour of the 316L grade, including the dissolution corrosion addressed in this study. The literature survey of the LMC behaviour of 316L and compositionally-similar steels (e.g., 316, 1.4571, 304L) in contact with liquid LBE revealed that, even though dissolution corrosion can occur locally at oxygen-saturated LBE and at temperatures as low as 400 °C, it becomes particularly promoted at high temperatures ($T \geq 450$ °C) and low LBE oxygen concentrations ($C_O < 10^{-8}$ mass%) [5,12–18,21–49]. Dissolution corrosion at elevated temperatures is promoted because the solubility of the main steel alloying elements (i.e., Ni, Cr, Fe) in the liquid LBE increases with temperature [50]. Low LBE oxygen concentrations favour dissolution corrosion by suppressing the formation of protective oxide scales. Based on the above, this study exposed 316L steels to oxygen-poor, static LBE ($C_O < 10^{-8}$ mass%) at 500 °C to ensure the manifestation of dissolution corrosion. Despite the aggressive exposure conditions, the relevance of this study for the development of MYRRHA is manifold: first, one cannot exclude high-temperature transients ($T \geq 500$ °C) during the system operation or oxygen-depleted zones of static LBE, i.e., similar service conditions as those tested here; second, the oxide scale might lose its local protectiveness with time due to chemical or mechanical damage, resulting in local dissolution attack [12,13,51,52]; third, the adopted testing approach allows the assessment of the maximum dissolution rate, which is important for establishing safety margins for the reliable use of thin-walled components.

This study aims at the in-depth understanding of the 316L steel dissolution corrosion behaviour in the absence of a protective oxide, an event that cannot be excluded in a real system, at least locally. To make this work relevant for the 316L steel grade and not for a single steel heat only, different heats must be simultaneously exposed to the same exposure conditions, so as to study the effect of the steel thermomechanical state and microstructure on its dissolution corrosion behaviour. This know-how is not only valuable for the optimum design of nuclear systems, such as MYRRHA, but also in view of the scarcity of studies addressing the effect of microstructure and thermomechanical state of the 316L steel grade on its compatibility with LBE.

2. Experimental

2.1. Materials

Three different 316L austenitic stainless steel heats (1 solution-annealed, 2 cold-drawn) were exposed to oxygen-poor static liquid LBE in this work. The solution-annealed heat, henceforth

designated 316LSA, was a plate (15 mm thickness; EUROTRANS-DEMETER heat [53]; Industeel, ArcelorMittal, S.A.) solution-annealed in the 1050–1100 °C range, followed by a water quench. The cold-drawn steel heats, henceforth designated 316LH1 (Aceros Inoxidables OLARRA, S.A.) and 316LH2 (Sidero Staal nv), were cylindrical rods (\varnothing 10 mm): 316LH1 was solution-annealed at 1060 °C for 4 h and water-quenched prior to cold deformation, while the heat treatment of 316LH2 was not provided by the steel supplier. Usually, solution annealing of austenitic stainless steels is conducted above 1040 °C for short times (several minutes) to bring chromium carbides into solution in the austenite and control grain growth [54]. The degree of cold work of 316LH1 and 316LH2 heats was not provided by the suppliers. Table 1 shows that the chemical compositions of the three heats agreed with the AISI 316L grade specification.

The microstructure of the as-received steel heats was first assessed by light optical microscopy (LOM) on steel specimens that were chemically etched with Carpenters' reagent (8.5 g FeCl₃, 2.4 g CuCl₂, 122 ml HCl, 6 ml HNO₃, 122 ml ethanol) for ~1 min. LOM images of etched 316LSA, 316LH1 and 316LH2 samples are shown in Fig. 1. The average grain size of the three steels was: 45 μ m in 316LH1, 65 μ m in 316LH2, and varied locally between 30 and 45 μ m in 316LSA. The cold-drawn heats 316LH1 and 316LH2 exhibit deformation twins and other features typical for cold-deformed steels. The solution-annealed 316LSA heat shows δ -ferrite stringers parallel to the rolling direction. The phase composition of the as-received 316L steels was determined by X-ray diffraction (XRD; Seifert 3003, GE), using a Cu K α radiation source (operating conditions: 40 kV, 40 mA). The XRD patterns (Fig. 2) were acquired in the 30–90° 2 θ range with a step size of 0.02° and a time of 2s per step. The only identified phase in all heats was austenite (face-centred cubic, fcc; Fm $\bar{3}$ m; JCPDS file: 01-071-4649) except for solution-annealed 316LSA, which contained a small fraction of α -ferrite (body-centred cubic, bcc; Im $\bar{3}$ m; JCPDS file: 03-065-4899). α -ferrite results from the low-temperature (727–738 °C) transformation of its high-temperature (>1394 °C) polymorph δ -ferrite that is retained in the steel microstructure even after the solution annealing treatment [54,55]. The term δ -ferrite is herein used to denote the high-temperature origin of this steel precipitate.

The microstructure of the as-received cold-drawn steels was characterised on the nanoscale by means of transmission electron microscopy (TEM). The TEM (JEM-3010, JEOL, Japan) was operated at 300 kV using a side-entry type double tilt specimen holder with angular ranges of $\pm 30^\circ$. Samples for TEM investigation were prepared from \varnothing 3 mm disks punched out of a thin steel slab (~200 μ m). These were mechanically polished to 100–130 μ m thickness and electropolished to perforation in a Struers Tenupol 3 (operating conditions: 30 V, 0.2 A, –40 °C), using an electrolyte made of 95% CH₃OH (methanol) and 5% HClO₄ (perchloric acid).

Fig. 3 shows the two main modes of plastic deformation encountered in all thin foils extracted from the cold-drawn steels,

Table 1

Comparison of the chemical composition of the 316LSA, 316LH1 and 316LH2 steel heats to the AISI 316L chemical specification. All elemental concentrations are in mass%; the balance is Fe.

Element	316LSA	316LH1	316LH2	AISI 316L
C	0.019	0.028	0.022	≤ 0.03
Si	0.67	0.34	0.51	≤ 0.75
Mn	1.81	1.85	1.58	≤ 2.0
P	0.032	0.033	0.029	≤ 0.045
S	0.004	0.027	0.016	≤ 0.03
Cr	16.73	16.7	16.0	16.0–18.0
Ni	9.97	10.1	10.1	10.0–14.0
Mo	2.05	2.06	2.1	2.0–3.0

Download English Version:

<https://daneshyari.com/en/article/5454014>

Download Persian Version:

<https://daneshyari.com/article/5454014>

[Daneshyari.com](https://daneshyari.com)